Analysis of MCG with spatial filter method

K. Y. Sai[1], Y. Uchikawa[2], and M. Kotani[3]

[1]*Fukuda Denshi Technical Service Co.,LTD. Chiba 270-1495 Japan;*
[2]*Faculty of Science and Engineering, Tokyo Denki University, Hatoyamacho, Hikigun, Saitama, Japan;*
[3]*Department of Electronic Engineering, Tokyo Denki University, 2-2, Kanda-Nishiki-cho, Tokyo, Japan*

1 Introduction

Magnetocardiogram (MCG) mapping is a new promising non-invasive tool for obtaining functional information concerning the electrical activities of the heart. Since MCG was first measured by Baule and McFee[1], the MCG has been studied worldwide. In particular, it is known that Cohen and his co-workers measured the MCG by use of a SQUID inside a magnetically shielded room[2] and the technique has been applied to the localization of various bio-electric events in the heart, such as the ventricular preexcitation site in Wolff-Parkinson-White (WPW) syndrome patients[3,4], or the late depolarization activity in arrhythmogenic tissue[5,6]. However, MCG has not been widely applied in clinics because the method for obtaining an MCG is cumbersome and the liquid helium coolant is expensive. For these reasons, high-Tc SQUID has been receiving attention as a diagnostic technique for observing the electrical activities of the heart.

In the measurement of the High-Tc SQUID, the sensitivity is lower than the Low-Tc SQUID and the surrounding noise and the measurement errors will easily influence measured results and estimation of signal source. We try to use the spatial filter method (SFM) in signal analysis of MCG to reduce the influence of noise. The results were very satisfactory.

In this paper, a 16-channel high-Tc SQUID magnetometer was used in the measurement of the current dipole and MCG of ten normal subjects and four patients with myocardial infarction. The results of the simulation and actual measurement demonstrate the SFM method is useful for researching of biomagnetic signals and is helpful in reducing the influence of noise and signal source error.

2 Methods

2.1 Spatial filter and spatial frequency

An ideal filter should pass the desired frequency components and cut off other frequency components[7]. In the measurement of the biomagnetic signal, the ideal filter should permit the biomagnetic signal passage only and cut off other high frequency noise. This can raise the accuracy in estimation of the signal source. Because the biomagnetic signal is distributed in space, it is necessary to use the spatial filter.

When the spatial filter is used, the choice of the maximum frequency, suitable cut off frequency and the distance between two measurement points are very important. According to Biot-Savart equation we can obtain a magnetic field distribution that is produced by a current dipole (see Fig.1).

In Fig.1, *Bz* is the magnetic field produced from the current dipole. *Idl* is the current dipole moment. *Z* is the distance from the current dipole to measurement point. The magnetic field *Bz* changes with x.

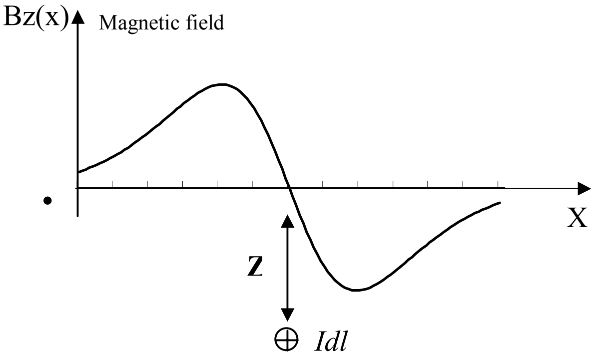

Figure 1: *The magnetic field produced by the dipole.*

To obtain the maximum frequency and the interval between the measurement points, we apply FFT to Fig.1. Here, we set depth (*Z*) as 6 cm (distance between dipole and sensor), *I* is 1 mA and *dl* is 5 mm. Fig.2 shows a curve after FFT. We obtain the

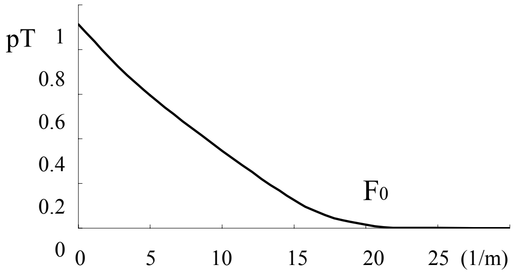

Figure 2: *Frequency curve after passed FFT.*

maximum frequency (F_0) as F_0=20 (1/m) from Fig.2. When we change the distance Z, the maximum frequency will vary also.

To recover the original wave of the magnetic field distribution of Bz, according to the sampling theorem, the interval of the measurement points must be smaller than $1/2F_0$.

Next we describe the spatial filter interpolation. When a pulse signal containing all frequency components passes through a low pass filter, frequency components higher than cut by cut off frequency (Fw) are eliminated. If a maximum frequency component (F_0) including noise passes an ideal spatial filter, the noise will be removed beyond the cut off frequency Fw. Therefore, selecting a suitable cut off frequency (Fw) to carry out filtering is very important. Here, we can obtain different interpolations using sampling function shown in equation (1). Fig.3 shows the calculated result using different Fw.

$$Bz(x) = \sum_{i=1}^{n} (Bz_i \times Fw \frac{Sin 2\pi Fwx}{2\pi Fwx}) \qquad (1)$$

Here, Fw is the cut off frequency of the low pass filter. From Fig.3, we observe the variation of the approximation curve when Fw change.

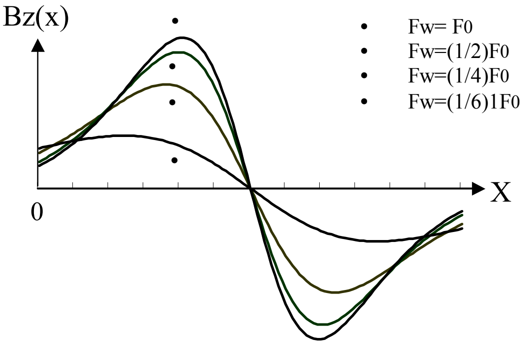

Figure 3: *Approximation curves of magnetic field measured at each point by changing Fw.*

2.2 Computer simulation

One current dipole and sixteen sensors are assumed. The dipole is assumed in the lower middle of the measurement plane and the distance to the nearest sensor is Z=60mm. The current is set as 1mA and the angle of the current dipole is set as -60 degree. Here, the magnetic field produced by the dipole is presumed in the x and y plane. The angle of dipole is measured from the positive x axis in counter-clockwise direction. Then, we added an error noise of 10% of the calculated magnetic field (Bz) at each measured point.

Simulation is performed for a variety Fw of the spatial filter. Because our analyses are based on 2-D data, the results are shown in the isofield map.

Fig.4 shows the filtered results using different Fw. In the isofield, the fixed circles are measurement points. The broken line is the positive magnetic field (source) and the solid line is the negative magnetic field (sink). A thick line is zero line (boundary line). The x axis and y axis are 20 cm long. When the value of Fw is reduced (from F_0 to $1/10\ F_0$), the curves of the isofield map become smoother, but the dipole deduced also vary.

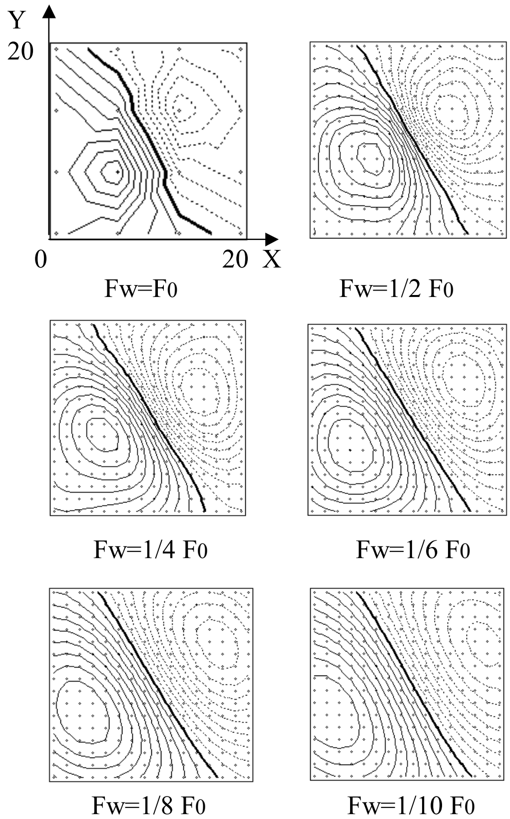

Figure 4*: Isofield map of filtering using different Fw.*

According to Biot-Savart rule, we can estimate the site and strength of the current dipole. Table 1 shows the result for different Fw. To compare the simulation results, we used equation (2) to calculate goodness of fit (GOF) in the strength of the magnetic field deduced

$$goodness\ of\ fit = \left[1 - \frac{\sum_{i=1}^{N} (Bzi - \tilde{B}zi)^2}{\sum_{i=1}^{N} Bzi^2} \right] \times 100\% \qquad (2)$$

Where the N is the number of measurement points, Bzi is the value of filtered the magnetic field and $\tilde{B}zi$ is the theoretical value.

From Table 1, we observe that the GOF ranges from 93.55% to 99.88% when Fw are changes from 1/2 F_0 to 1/10 F_0 (except Fw = F_0). But, when Fw is 1/4 F_0, the GOF reaches the highest value (99.88%). Furthermore, we observe that the result of estimation is sufficiently close to the theoretical values in position, direction and magnetic field.

Table 1: *The results of deduced after changing Fw.*

Fw : F_0	ZL	θ	IDL	GOF
Theoretical values	[mm] 60	[°] -60	[A*m] 6.03E-7	[%] 100
Fw =F_0	40	-45	4.61E-7	87.33
Fw =1/2 F_0	48	-56	3.80E-7	96.72
Fw =1/4 F_0	59	-58	5.85E-7	99.88
Fw =1/6 F_0	64	-61	6.54E-7	99.75
Fw =1/8 F_0	77	-66	6.61E-7	99.55
Fw =1/10F_0	93	-67	6.52E-7	93.55

3 MCG measurement

3.1 Measurement method

The MCG of ten normal subjects and four patients with myocardial infarction were measured. The 16-channel high-Tc SQUID magnetometer is set on the anterior chest wall about 40 mm apart. Fig.5 shows the measurement grid on the anterior chest wall.

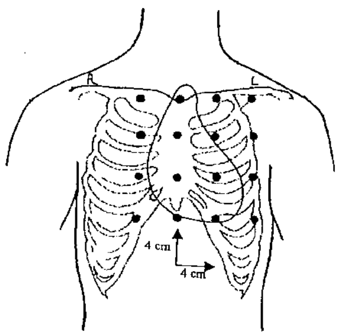

Figure 5: *The measurement grid of MCG on the subject.*

The output signal from the magnetometer was processed by the Flux Locked Loop circuit and only retained the frequency band 0.05~100 Hz. Then the signals were digitized with a 12-bit A/D converter using a sampling rate of 1000 Hz[8]. Finally the digital signals were averaged by 160 measurements in one position.

3.2 Measurement results

Fig.6 shows isofield maps of a normal subject at 10 ms from onset of the QRS wave (the highest point of R wave) before and after using the spatial filter. Here, the setting of the isofield maps is the same as Fig.4. The cut off frequency Fw is 1/4 F_0. In the normal subjects, the result deduced after filtering shows the signal source is located 75±10 mm under the anterior chest wall, and the angle is 170±10 degree. Because of the error existed, the result shows some difference. We observe the magnetic field vary with the deduced depth of the signal source.

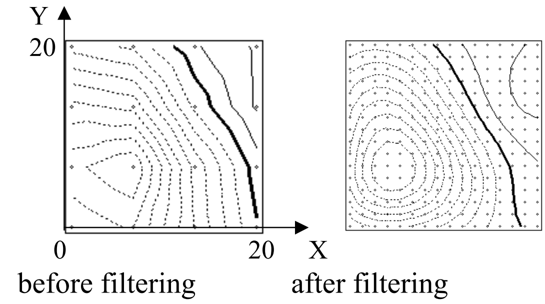

Figure 6: *The isofield maps of a normal subject.*

Fig.7 shows the isofield map of the patient with myocardial infarction subject at 10 ms from onset of the QRS wave (the highest point of R wave) before and after using the spatial filter. Though the trigger time is the same as the normal subjects, the position and angle of the signal source deduced show different result.

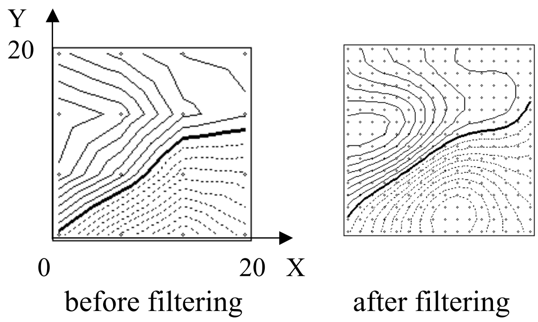

Figure 7: *The isofield maps of a patient with myocardial infarction.*

From Table 2, w observe the depth of the signal source is 80±10mm and the angle is 120±5. No.4 patient (P4) shows quite different signal source

Table 2: *The results deduced for four patients.*

	Position (mm)	θ (degree)	depth (cm)	magnetic field (T)
P1	11.3, 13.2	123	86.7	1.09E-12
P2	10.5, 14.1	124	73.5	0.72E-12
P3	11.4, 15.1	118	89.3	0.68E-12
P4	10.1, 7.6	57	100.	2.54E-12

because the infarct position of this patient is different from other patients.For the patient with myocardial infarction, the vector of the injury current will be produced in the infarct position. The vector influences the normal vector of the heart[9,10]. We can deduce the direction and depth of the signal source using the MCG measured, and then apply to diagnosis of disease according to variance of the signal source.

4 Conclusions

The high-Tc SQUID has been receiving attention because the low cost and simple operation in the measurement of MCG. We carried out the MCG measurement in the normal subjects and the patients using a 16 channel high-Tc SQUID. The result shows the high-SQUID is applicable in MCG. The position and depth of the signal source can be deduced using the MCG. It will provide some assistance in the diagnosis of cardiac diseases.
Though the sensitivity of the High-Tc SQUID is lower than the Low-Tc SQUID and the surrounding noises will easily influence measurement. We used the spatial filter method to process the signal of the MCG. The result shows the method is useful for reducing the noise and increasing the accuracy in the estimation of the signal source. The method applies in other biomagnetic signals.

The spatial filtering method based on the sampling theorem has been used in 16 channel High-Tc in our research. It is expected to develop the application of the SFM in the multi channel system in future.

References

1. G.M. Baule and R. McFee, “Detection of the magnetic field of the heart”, *Am Heart J.* **66**, 95, 1963.
2. D. Cohen, E.A. Edelsack, and J.E. Zimmerman, “Magnetocardiograms taken inside a shielded room with a superconducting point-contact magnetometer”, *Appl Phys Lett.* **16**, 278, 1970.
3. S.N. Erne, “High resolution magnetocardio-graphy Modeling and source localization”, *Med.Biol.Eng.* **23**, 1447-1450, 1985.
4. Y. Uchikawa and S.N. Erne, “Modelling the Wolff-Parkinson-White syndrome for magneto-cardiography”, in *Biomagnetism ’87,* 1988, pp. 322.
5. R.R. Fenici, M. Masselli, L. Lopez, and G. Mellillo, “Magnetocardiographic localization of arrhythomogenic tissue”, in *Biomagnetism ’87.* 1988, pp. 282-285.
6. K. Fujino, M. Sumi. K. Saito, M. Murakami, T. Higuchi, Y. Nakaya and H. Mori, “Magnetocardiograms of patients with left ventricular overloading recorded with a second-derivative SQUID gradiometer”, *J. Electro-cardiol.* 219, 1984.
7. J. Nenonen, T. Katila, M. Leiniö, J. Montonen, M. Mäkijärvi, and P. Siltanen, “Magnetocardio-graphic functional localization using current multipole models”, *IEEE.Trans.Biomed.* 5421-5427, 1991.
8. M. Nomura, T. Saijyo, Y. Haruta, and H. Itozaki, “Biomagnetic measurement of gastric mechanical motility using a high-temperature SQUID imaging”, *Biomag96: Tenth International Conference on Biomagnetism,* 1996, pp. 181-184.
9. O. Mituharu, “Computer diagnosis of ECG”, *Nakayama Shoten Co., Ltd*. 1989, pp. 195-204.
10. K. Kanzi and Y. Kobayasi, “ABC of ECG”, *Doctor academy of Japan*. 1992, pp. 218-220.